



Transistor application of single crystals of [8]phenacene

Journal:	<i>Journal of Materials Chemistry C</i>
Manuscript ID:	TC-ART-04-2015-000960.R1
Article Type:	Paper
Date Submitted by the Author:	03-Jun-2015
Complete List of Authors:	<p>Shimo, Yuma; Okayama University, Department of Electric and Electronic Engineering Mikami, Takahiro; Okayama University, Department of Electric and Electronic Engineering Murakami, Hiroto; Okayama University, Department of Electric and Electronic Engineering Hamao, Shino; Okayama University, Research Laboratory for Surface Science Goto, Hidenori; Okayama University, Research Laboratory for Surface Science Okamoto, Hideki; Okayama University, Chemistry Goda, Shin; NARD Institute, Ltd., Sato, Kaori; NARD Institute, Ltd., Cassinese, Antonio; University of Naples, Department of Physics Hayashi, Yasuhiko; Okayama University, Department of Electric and Electronic Engineering Kubozono, Yoshihiro; Okayama University, Research Laboratory for Surface Science</p>

ARTICLE

Transistor application of single crystals of [8]phenacene

Cite this: DOI: 10.1039/x0xx00000x

Yuma Shimo,^a Takahiro Mikami,^a Hiroto T. Murakami,^a Shino Hamao,^b Hidenori Goto,^b Hideki Okamoto,^c Shin Gohda,^d Kaori Sato,^d Antonio Cassinese,^e Yasuhiko Hayashi^a and Yoshihiro Kubozono^{*bfg}

Received 00th January 2012,
Accepted 00th January 2012

DOI: 10.1039/x0xx00000x

www.rsc.org/

Field-effect transistors (FETs) with single crystals of a new phenacene-type molecule, [8]phenacene, were fabricated and characterized. This new molecule consists of a phenacene core of eight benzene rings, with an extended π -conjugated system, which was recently synthesized for use in an FET by our group. The FET characteristics of an [8]phenacene single-crystal FET with SiO₂ gate dielectrics show typical p-channel properties with an average field-effect mobility, $\langle\mu\rangle$, as high as 3(2) cm² V⁻¹ s⁻¹ in two-terminal measurement mode, which is a relatively high value for a p-channel single-crystal FET. The $\langle\mu\rangle$ was determined to be 6(2) cm² V⁻¹ s⁻¹ in four-terminal measurement mode. Low-voltage operation was achieved with PbZr_{0.52}Ti_{0.48}O₃ (PZT) as the gate dielectric, and an electric-double-layer (EDL) capacitor. The $\langle\mu\rangle$ and average values of absolute threshold voltage, $\langle|V_{th}|\rangle$, were 1.6(4) cm² V⁻¹ s⁻¹ and 5(1) V, respectively, for PZT, and 4(2) x 10⁻¹ cm² V⁻¹ s⁻¹ and 2.38(4) V, respectively, for the EDL capacitor; these values were evaluated in two-terminal measurement mode. The inverter circuit was fabricated using [8]phenacene and *N,N'*-1*H,1H*-perfluorobutyldicyanoperylene-carboxydi-imide single-crystal FETs. This is the first logic gate circuit using phenacene molecules. Furthermore, the relationship between μ and number of benzene rings was clarified based on this study and the previous works on phenacene single-crystal FETs.

Introduction

Organic single-crystal field-effect transistors (FETs) have been extensively studied because of their high field-effect mobilities, μ 's, and utility as a tool to improve understanding of the intrinsic nature of FETs.¹⁻¹¹ Extrinsic factors, such as grain boundaries and defects, which can dominate the characteristics of an FET, can be eliminated when single crystals are used as active layers; a single crystal is ideally free of grain boundaries and defects. The first success in FET operation of a single-crystal FET goes back to 2003. Takeya *et al.* fabricated a pentacene single crystal FET with the μ of 0.5 cm² V⁻¹ s⁻¹,¹ while Podzorov *et al.* fabricated a rubrene single-crystal FET that showed excellent FET characteristics ($\mu \sim 8$ cm² V⁻¹ s⁻¹).² The μ value currently reaches 40 cm² V⁻¹ s⁻¹ for a rubrene single-crystal FET in four-terminal measurement mode, and 18 cm² V⁻¹ s⁻¹ in two-terminal measurement mode.³ The highest μ value realized in an organic single-crystal FET is 94 cm² V⁻¹ s⁻¹ in κ -(BEDT-TTF)₂Cu[N(CN)₂Br] (BEDT-TTF: bis(ethylenedithio)tetrathiafulvalene).⁴ An organic single-crystal FET generally shows a higher μ value than an organic thin-film FET, although the high μ values were recently

reported, such as 43 cm² V⁻¹ s⁻¹ for a thin-film FET of 2,7-dioctyl[1]benzothieno[3,2-*b*][1]benzothiophene (C8-BTBT),¹² and 20.9 cm² V⁻¹ s⁻¹ for a thin-film FET of 3,10-ditetradecylpicene (picene-(C₁₄H₂₉)₂)¹³ which consists of a phenacene core with five benzene rings and two alkyl chains.

Recently, our group has fabricated thin-film and single-crystal FETs with phenacene-type molecules, which have W-shaped structures consisting of benzene rings.¹³⁻²⁰ Most phenacene thin-film FETs^{13-16,18} show μ values above 1 cm² V⁻¹ s⁻¹. The thin-film FET based on [6]phenacene, which has six benzene rings, showed a μ as high as 7.4 cm² V⁻¹ s⁻¹ (ref. 16), and a single-crystal FET with [7]phenacene, with its seven benzene rings, exhibited a μ as high as 6.9 cm² V⁻¹ s⁻¹ (ref. 20). Thus, very high μ values are realized in FETs with phenacene-type molecules even without alkyl side chains. Very recently, we synthesized the [8]phenacene molecule, with eight benzene rings, and used it to fabricate a thin-film FET.¹⁸ The μ value was 1.74 cm² V⁻¹ s⁻¹ in the FET with SiO₂ gate dielectrics.

Presently, the highest μ value for a phenacene single-crystal FET is from [7]phenacene (6.9 cm² V⁻¹ s⁻¹)²⁰, but the μ value from a [6]phenacene single-crystal FET is too low (lower than 1 cm² V⁻¹ s⁻¹), probably due to the poor quality of the crystals,

despite the high μ value seen in a [6]phenacene thin-film FET.¹⁶ Sufficiently large single crystals of [6]phenacene could not be obtained,¹⁷ so the μ of the [6]phenacene single-crystal FET was low, but that of the [7]phenacene single-crystal FET was excellent. In addition, the μ value in the [6]phenacene single-crystal FET was lower than that ($1.3 \text{ cm}^2 \text{ V}^{-1} \text{ s}^{-1}$)¹⁹ in a picene single-crystal FET. It is natural that [8]phenacene should be investigated as the next target molecule for a single-crystal FET. More extended phenacene molecules like [8]phenacene may benefit from an increase in the transfer integral between the molecules, because of the increased π - π stacking between molecules through the extended π -framework. However, it may not be simple to determine whether the extended π -framework is what is responsible for the larger transfer integral since the C-H...C interaction between molecules also plays an important role in molecular stacking. Furthermore, the molecular symmetry of phenacenes with odd and even numbers of benzene rings is different (C_{2v} for odd and C_{2h} for even), and FET properties may be found that differ for odd and even numbers (or the parity effect), as is expected from the variation of the μ values in single-crystal FETs with picene (odd),¹⁹ [6]phenacene (even)¹⁷ and [7]phenacene (odd)²⁰. But first, the [8]phenacene single-crystal FET had to be fabricated to clarify these questions and help formulate a strategy to realize excellent FET performance using benzene-network molecules.

In this study, we fabricated [8]phenacene single-crystal FETs with SiO_2 and $\text{PbZr}_{0.52}\text{Ti}_{0.48}\text{O}_3$ (PZT) gate dielectrics as well as an EDL capacitor with an ionic liquid polymer ([1-butyl-3-methylimidazolium][hexafluorophosphate] (bmim[PF₆])) sheet. Their FET properties were fully investigated in two- and four-terminal measurement modes at room temperature. The single crystals of [8]phenacene showed the very thin planar form that is suitable for an FET device. The crystals are colourless and transparent. Furthermore, for low-voltage operation and the accumulation of a high density of carriers, [8]phenacene single-crystal FETs with PZT gate dielectrics and EDL capacitors were fabricated and their low-voltage FET performance was confirmed. The inverter circuit was also fabricated using [8]phenacene and *N,N'*-1*H*,1*H*-perfluorobutylidicyanoperylene-carboxydi-imide (PDIF-CN₂) single-crystal FETs and the successful operation was confirmed.

Results

Characterization of single crystals of [8]phenacene

Single crystals of [8]phenacene were fabricated by physical vapour transport (PVT, experimental details in the experimental section). Optical photographs and atomic force microscopy (AFM) images of [8]phenacene single crystals are shown in Fig. 1a. The transparent plate-type single crystals are shown in the optical photograph. The photograph is quite similar to that of [8]phenacene single-crystal prepared preliminary in our previous paper (see Fig. S10 of ref. 18). The AFM image shows

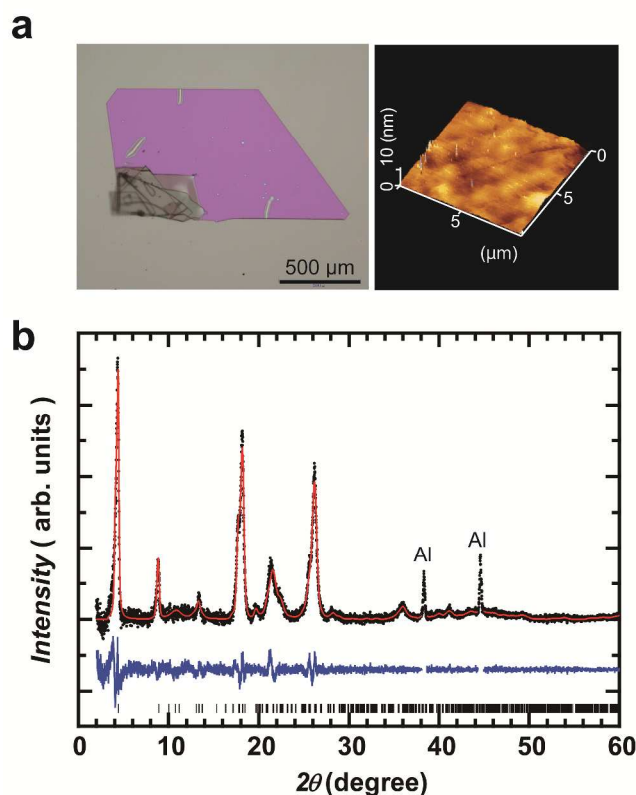


Fig. 1 (a) Optical micrograph and AFM image of single crystals of [8]phenacene. (b) XRD pattern of powder sample of [8]phenacene. Dots (black) and solid lines (red) refer to the experimental and calculated (LeBail fit) patterns. The difference between experimental and calculated patterns and the predicted reflections are shown as lines (blue) and ticks (black), respectively.

the one-layer scale roughness ($\sim 0.5 \text{ nm}$) on the surface of a single crystal, *i.e.*, it is a very flat surface.

We tried to measure the X-ray diffraction (XRD) data using single crystals of [8]phenacene, but no sufficient number of Bragg reflections were collected because of very thin single crystals (plate-type shape). Therefore, the obtained single crystals were ground to obtain a white crystalline-powder, and their powder XRD pattern was analysed. Fig. 1b displays the XRD pattern of the polycrystalline powder sample of [8]phenacene. The XRD pattern is similar to those of picene²¹ and [7]phenacene,¹⁷ implying structural similarity. LeBail fitting for the XRD pattern was achieved with the space group $P2_1$ (monoclinic lattice) to determine the lattice constants. The a , b , c and β are listed in Table S1 of ESI[†], together with those of other phenacene molecules. Only $00l$ reflections were observed from a thin film of [8]phenacene (not shown), which is the same as previously found¹⁸. This means that the thin film grows parallel to the surface of the SiO_2 gate dielectric. The average distance between the ab -planes, $\langle d_{001} \rangle$ ($= 1/|c^*|$), of the powder sample increases linearly with increasing number of benzene rings (not shown), which is almost the same as the $\langle d_{001} \rangle$ against number of benzene rings in [8]phenacene thin-films (Fig. 3b of ref. 18), and the c value of [8]phenacene lies on a straight line (not shown), implying the successful synthesis

of [8]phenacene, and indicating the similar β values in all phenacenes (see Table S1 of ESI[†]). A tilt angle of 25° with respect to c^* was calculated by considering the $\langle d_{001} \rangle$ and van der Waals size of [8]phenacene (long-axis). c^* refers to the reciprocal vector of c where $c = |c|$. The evaluated tilt angle for the powder sample is slightly larger than that, 20°, determined with the thin-film of [8]phenacene by our group.¹⁸

FET characteristics of an [8]phenacene single-crystal FET

The FET characteristics of [8]phenacene single-crystal FETs were measured in two-terminal measurement mode. 300-nm thick SiO₂ gate dielectrics are used in this FET device, and the surface of the SiO₂ gate dielectrics is covered with 30-nm thick parylene. Fig. 2a shows a schematic representation to explain the measurement mode. The transfer and output curves are shown in Fig. 2b and c, respectively. Typical p-channel normally-off FET characteristics are observed. The FET parameters, μ , absolute threshold voltage $|V_{th}|$, on-off ratio and sub-threshold swing (S) were determined from the forward transfer-curve (Fig. 2b) in the saturation regime ($V_D = -100$ V) using the general MOS formula.²² The μ , $|V_{th}|$, on-off ratio and S were 8.2 cm² V⁻¹ s⁻¹, 28 V, 3.5 × 10⁸ and 1.6 V decade⁻¹, respectively; the parameters were obtained from the steepest transfer curve observed in the low absolute gate voltage, $|V_G|$, region (40–60 V). Furthermore, the μ and $|V_{th}|$ were determined to be 5.7 cm² V⁻¹ s⁻¹ and 22 V from the transfer curve in the high- $|V_G|$ region (70–80 V), exhibiting a slower increase. Therefore, the μ value is still high even in the high- $|V_G|$ range. Thus, the [8]phenacene single-crystal FET shows excellent FET characteristics. The FET parameters for eighteen FET devices fabricated in this study are listed in Table S2 of ESI[†]; device 13 in Table S2 provided Fig. 2b and c. The average μ , $\langle \mu \rangle$, value was 3(2) cm² V⁻¹ s⁻¹, estimated from eighteen FETs, which also means excellent performance.

Here, we must comment the relatively high $|V_{th}|$'s in the above FET, which is generally observed in phenacene thin-film and single-crystal FETs. When the gate dielectric is changed from SiO₂ ($C_o = 10.4$ nF cm⁻²) to the high- k gate dielectric ($C_o = 62.5$ nF cm⁻²), the $|V_{th}|$ decreases from 26 to 5 V, which is reasonable. However, the $|V_{th}|$ may be relatively high in comparison with other organic FETs. This is the characteristics of phenacene FETs, although the exact origin is still unclear. We speculate that the structure and morphology of phenacene molecules on gate dielectric may relate to it.

It should be noted on the basis of the data listed in Table S2 that the μ value tends to increase with increasing channel length L . The average value of $\langle \mu \rangle$ was evaluated individually from each FET with different L 's. Here, $\langle \mu \rangle$ was plotted as a function of L , showing a linear relation (Fig. S1). This implies the influence of contact resistance R_c in the FET.

We tried to evaluate the contact resistance based on 'transfer length method (TLM)'. Fig. 3 shows the $RW - L$ plot of [8]phenacene single-crystal FET with SiO₂ gate dielectric, where the two-terminal resistance, R , was obtained from the slope of $|I_D| - |V_D|$ in the linear region ($|V_D| = 10 - 20$ V) at $V_G = -100$ V. Clear linear relationship was obtained in the $RW - L$ plot, which is reasonable because RW is expressed as ' $RW = R_{ch}W + 2R_cW = \rho_{ch-sheet}L + 2R_cW$ ' where $\rho_{ch-sheet}$ and R_{ch} are 'sheet resistance' and 'resistance' of channel region. From an

intercept, $2R_cW$, was determined to be 3(1) × 10³ Ω cm, *i.e.*, for $W = 300$ μm, $R_c = 50$ kΩ, while $\rho_{ch-sheet}$ was evaluated to be 3.4(7) × 10² kΩ from the slope of $RW - L$ plot. The $R_{ch}W$ is almost the same as $2R_cW$ at $L = 100$ μm (see Fig. 3), but at $L = 200$ μm, $2R_cW$ is 1/2 of $R_{ch}W$. Namely, an FET with a small L is significantly affected by contact resistance. In other words, the fraction by which contact resistance affects FET performance is higher with a smaller L .

In this device (Fig. 2a), we inserted a 3 nm film of an electron-acceptor, 2,3,5,6-tetrafluoro-7,7,8,8-tetracyanoquinodimethane (F₄TCNQ), to reduce the contact resistance between source/drain electrodes and the single crystal; the effectiveness of lowering the contact resistance was confirmed in a [7]phenacene single-crystal FET.²⁰ However, the contact resistance here still remained, as suggested by the L -dependence of $\langle \mu \rangle$ (Fig. S1 of ESI[†]) and RW (Fig. 3). The $\langle \mu \rangle$ of the [8]phenacene single-crystal FETs with $L = 450$ μm reached 6(2) cm² V⁻¹ s⁻¹.

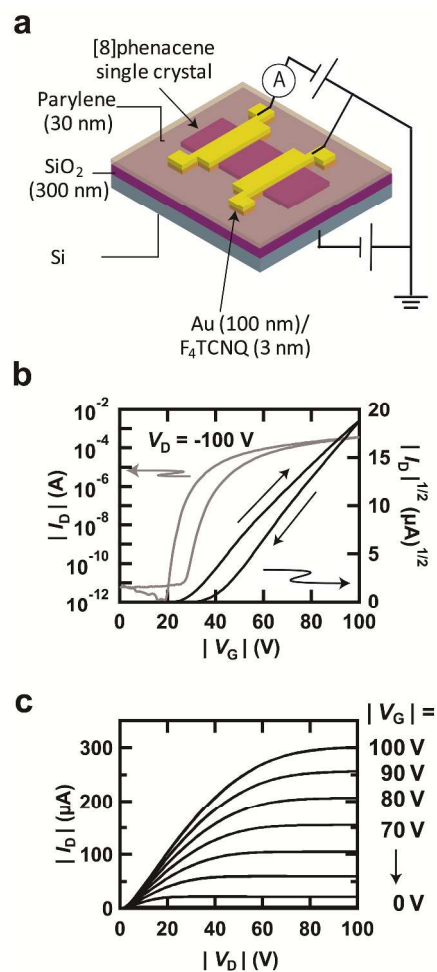


Fig. 2 (a) Schematic representation of two-terminal measurement mode and device structure of [8]phenacene single-crystal FET. (b) Transfer and (c) output curves of [8]phenacene single-crystal FET with SiO₂ gate dielectrics measured in two-terminal measurement mode.

Consequently, we must use larger L 's for the channel of the [8]phenacene single-crystal FET in addition to the insertion of F₄TCNQ, to fabricate a high-performance single-crystal FET. The output curves shown in Fig. 2c show typical p-channel normally-off output curves, in which the linear and saturation behaviours were recorded in the low absolute drain voltage ($|V_D|$) and the high $|V_D|$ regime, respectively. The concavity that is characteristic of contact resistance is noticeable in the output curves.

Next we treated the surface of the SiO₂ (400 nm) with hexamethyldisilazane (HMDS) instead of parylene. In the case of the [8]phenacene thin-film FET, HMDS was used as a surface treatment to provide a hydrophobic surface. The transfer and output curves of an [8]phenacene single-crystal FET with HMDS-treated SiO₂ gate dielectrics are shown in Fig. S2 in ESI[†]. The μ , $|V_{th}|$, on-off ratio and S were 1.5 cm² V⁻¹ s⁻¹, 20 V, 1.6 × 10⁷ and 2.7 V decade⁻¹, respectively. The $\langle\mu\rangle$ for three FETs fabricated in this study was 1.3(2) cm² V⁻¹ s⁻¹, which is smaller than the 3(2) cm² V⁻¹ s⁻¹ of the [8]phenacene single-crystal FET with parylene-coated SiO₂ gate dielectrics. Nevertheless, the $\langle\mu\rangle$ value is higher than 1 cm² V⁻¹ s⁻¹. To sum up, the FET performance of [8]phenacene single-crystal FETs has been compared with that of [7]phenacene single-crystal FETs, which have shown the highest μ among the phenacene single-crystal FETs up to the present time.^{17,20}

FET characteristics measured in four-terminal measurement mode

In order to fully investigate the contact resistance between single crystal and source/drain electrodes, the transfer and output curves were measured in four-terminal measurement mode. The details of measurement are described in the experimental section. The $|I_D|$ vs $|V_G|$ recorded at low $|V_D|$, *i.e.*, in the linear regime, was plotted as the transfer curve, and the forward transfer curve was fitted using the MOS formula for the linear regime²² to determine the FET parameters. In this analysis, the difference between $|V_1|$ and $|V_2|$ shown in Fig. 4a, which refers to the difference in the voltages providing the potential drop in the channel region of the single crystal, are used instead of $|V_D|$. The transfer and output curves recorded in four-terminal measurement mode are shown in Fig. 4b and c, respectively. The μ , $|V_{th}|$, on-off ratio and S were 7.3 cm² V⁻¹ s⁻¹, 43 V, 2.8 × 10⁷ and 9.3 × 10⁻¹ V decade⁻¹, respectively, from the forward transfer curve (Fig. 4b). The $\langle\mu\rangle$ value evaluated from three devices using four-terminal measurement was 6(2) cm² V⁻¹ s⁻¹, which is larger than the 3(2) cm² V⁻¹ s⁻¹ seen in two-terminal measurement mode. All FET parameters evaluated in four-terminal measurement mode are listed in Table S3 of ESI[†]; FET number 2 in Table S3 provided Fig. 4b and c. The difference in $\langle\mu\rangle$ between two- and four-terminal measurement modes also suggests the presence of contact resistance in the [8]phenacene single-crystal FET with SiO₂ gate dielectrics. The output curve was plotted as $|I_D|$ vs. $|V_1| - |V_2|$ at each $|V_G|$, which shows typical output curves for four-terminal measurement mode, *i.e.*, at low $|V_G|$, $|V_1| - |V_2|$ is too

small to place the output curve in the saturation regime. It is reasonable not to observe any concavity in the output curves shown in Fig. 4c.

Low-voltage operation in an [8]phenacene single-crystal FET.

Fig. 5a and b show the transfer and output curves of an [8]phenacene single-crystal FET with PbZr_{0.52}Ti_{0.48}O₃ (PZT) gate dielectrics (thickness in 150 nm), in which the PZT is covered with 30-nm thick parylene. The FET characteristics were measured in two-terminal measurement mode. Both curves show p-channel normally-off FET characteristics. The operation voltage is much lower than that of an [8]phenacene single-crystal FET with SiO₂ gate dielectrics, as seen from Fig. 2b and 5a. The μ , $|V_{th}|$, on-off ratio and S were determined to be 2.1 cm² V⁻¹ s⁻¹, 4.9 V, 9.2 × 10⁶ and 4.0 × 10⁻¹ V decade⁻¹, respectively, from the forward transfer curve in the saturation regime. The μ is higher than 1 cm² V⁻¹ s⁻¹, and the $|V_{th}|$ (= 4.9 V) and S (= 4.0 × 10⁻¹ V decade⁻¹) are much lower than those ($|V_{th}|$ = 28 V and S = 1.6 V decade⁻¹) for the [8]phenacene single-crystal FET with SiO₂ gate dielectrics (Fig. 2b). This means that the [8]phenacene single-crystal FET with PZT gate dielectrics is promising for future practical electronics because of its low-voltage operation as well as its high μ , no hysteresis was observed in this FET. Table S4 of ESI[†] lists the FET parameters of five [8]phenacene single-crystal FETs with PZT gate dielectrics, which have different L values (see Table S4), though no clear L dependence of μ was observed; the FET providing Fig. 5a and b is No. 3 in Table S4. The $\langle\mu\rangle$ was evaluated to be 1.6(4) cm² V⁻¹ s⁻¹ from five devices, which is slightly smaller than the 3(2) cm² V⁻¹ s⁻¹ of the [8]phenacene single-crystal FET with SiO₂ gate dielectrics.

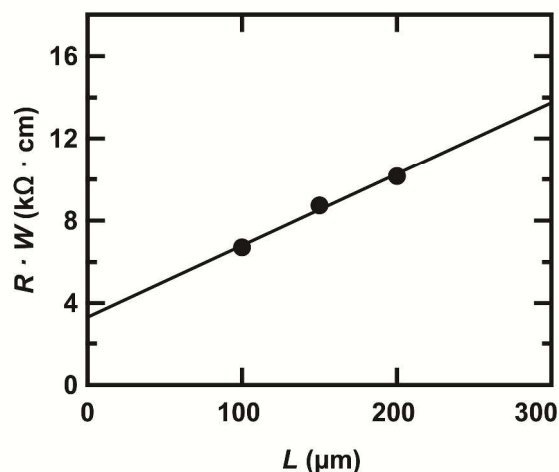


Fig. 3 L dependence of RW for [8]phenacene single-crystal FET with SiO₂ gate dielectric.

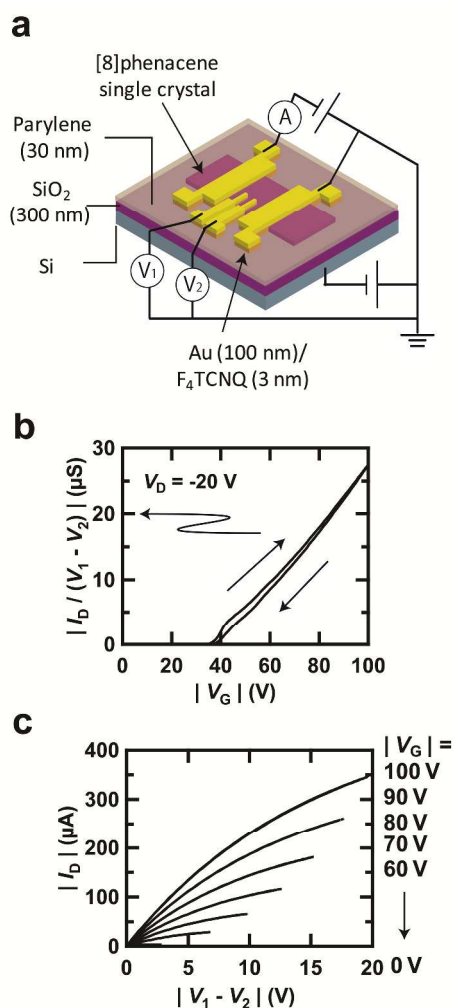


Fig. 4 (a) Schematic representation of four-terminal measurement mode and device structure of [8]phenacene single-crystal FET. (b) Transfer and (c) output curves of [8]phenacene single-crystal FET with SiO₂ gate dielectrics measured in four-terminal measurement mode.

FET characteristics of an [8]phenacene single-crystal FET with EDL capacitors

The transfer and output curves of the [8]phenacene single-crystal FET with EDL capacitors were measured in two-terminal measurement mode. A schematic representation of the measurements on the [8]phenacene single-crystal EDL FET is shown in Fig. 5c. The transfer and output curves are shown in Fig. 5d and e, respectively, which show p-channel FET properties. A bmim[PF₆] polymer sheet was used as the EDL capacitor in the FET. The transfer curve shows a rapid increase above 2 V. The μ , $|V_{th}|$, on-off ratio and S were determined to be $3.5 \times 10^{-1} \text{ cm}^2 \text{ V}^{-1} \text{ s}^{-1}$, 2.4 V, 3.8×10^2 and $5.2 \times 10^{-1} \text{ V decade}^{-1}$, respectively, from the forward transfer curve. The $\langle \mu \rangle$ was evaluated as $4(2) \times 10^{-1} \text{ cm}^2 \text{ V}^{-1} \text{ s}^{-1}$ from three EDL FETs. All FET parameters are listed in Table S5; FET number 2 provided Fig. 5d and e.

The hysteresis in the transfer curves is small in comparison with the normal transfer curves for the other phenacene single-crystal FETs with EDL capacitors.^{17,19} The observed $|V_{th}|$ listed in Table S5 of ESI[†] is smaller than the 3.5 – 6.1 V (Table S4) of devices with PZT gate dielectrics. This is owing to the larger C_o of an EDL capacitor, which is $7.86 \times 10^{-6} \text{ F cm}^{-2}$, compared with the $6.25 \times 10^{-8} \text{ F cm}^{-2}$ of PZT. Thus, the EDL capacitor produces high-density carrier accumulation even at low $|V_G|$ because of its high C_o . On the other hand, the μ value is much smaller than those of [8]phenacene single-crystal FETs with SiO₂ and PZT gate dielectrics. This is often found in FETs with high C_o ,^{17,19,23} and in particular the large surface roughness may suppress the μ in organic FETs with gate dielectrics possessing high C_o . To obtain a higher μ value, a large and smooth flat surface on the [8]phenacene single-crystals must be needed.

Fabrication of inverter circuit using [8]phenacene and PDIF-CN₂ single-crystal FETs

Inverter circuit was fabricated using [8]phenacene and PDIF-CN₂ single-crystal FETs. In this circuit, the former operates as p-channel FET, while the latter operates as n-channel FET. The constitution of inverter circuit is shown in Fig. 6a, together with the molecular structure of PDIF-CN₂. This type of inverter circuit is generally called ‘CMOS inverter’. The schematic representation of the inverter device fabricated is shown in Fig. 6b. The measurement mode is also shown in Fig. 6b. The transfer and output curves of typical PDIF-CN₂ single-crystal FET are shown in Fig. S3 of ESI[†]. The μ , $|V_{th}|$, on-off ratio and S of PDIF-CN₂ single-crystal FET were determined to be $1.3 \text{ cm}^2 \text{ V}^{-1} \text{ s}^{-1}$, -5.6 V, 1.8×10^2 and 14 V decade^{-1} , respectively, from the forward transfer curve in the saturation regime (Fig. S3). The μ value ($1.3 \text{ cm}^2 \text{ V}^{-1} \text{ s}^{-1}$) is twice higher than that ($0.6 \text{ cm}^2 \text{ V}^{-1} \text{ s}^{-1}$)²⁴ of its thin-film FET, and it is approximately a half of that ($2\text{--}3 \text{ cm}^2 \text{ V}^{-1} \text{ s}^{-1}$)²⁵ in the PDIF-CN₂ single crystal FET which was previously prepared using Cytop gate dielectric, showing a good performance.

The plot of output voltage, V_{out} , against input voltage, V_{in} , is shown in Fig. 6c; V_{out} and V_{in} are shown in Fig. 6a and b. As seen from Fig. 6c, at supply voltage, V_{DD} , of 100 V, the V_{out} is $\sim 100 \text{ V}$ at $V_{in} = 0 \text{ V}$. The V_{out} slightly decreases with increasing V_{in} , and it drastically decreases to reach 0 V at around 60 V. When decreasing V_{in} from 100 V, the V_{out} drastically increases to reach $\sim 100 \text{ V}$ below 70 V. Thus, $V_{out} \sim 100 \text{ V} = V_{DD}$ at low V_{in} , and $V_{out} = 0 \text{ V}$ at $V_{in} = 100 \text{ V} = V_{DD}$, i.e., inverter operation is confirmed. The hysteresis in the forward and reverse $V_{out} - V_{in}$ plots is a little observed for $V_{DD} = 100 \text{ V}$.

As seen from Fig. 6c, at all V_{DD} 's, $V_{out} \sim V_{DD}$ at low V_{in} , and $V_{out} = 0 \text{ V}$ at $V_{in} = V_{DD}$, i.e., inverter operation is observed. Threshold voltage of inverter circuit, V_{TIC} , should be $V_{DD}/2$ if the operation of both p-channel and n-channel FETs ideally balances. However, the V_{TIC} a little deviates from $V_{DD}/2$. The gain, $G_{inverter}$, of this circuit was evaluated from the slope of $V_{out} - V_{in}$ plot between 90% and 10% of V_{out} at $V_{in} = 0 \text{ V}$. The $G_{inverter}$ was 5.7 for $V_{DD} = 100 \text{ V}$. The maximum $G_{inverter}$ value of 7.1 was obtained for $V_{DD} = 60 \text{ V}$ in this inverter. The value is still

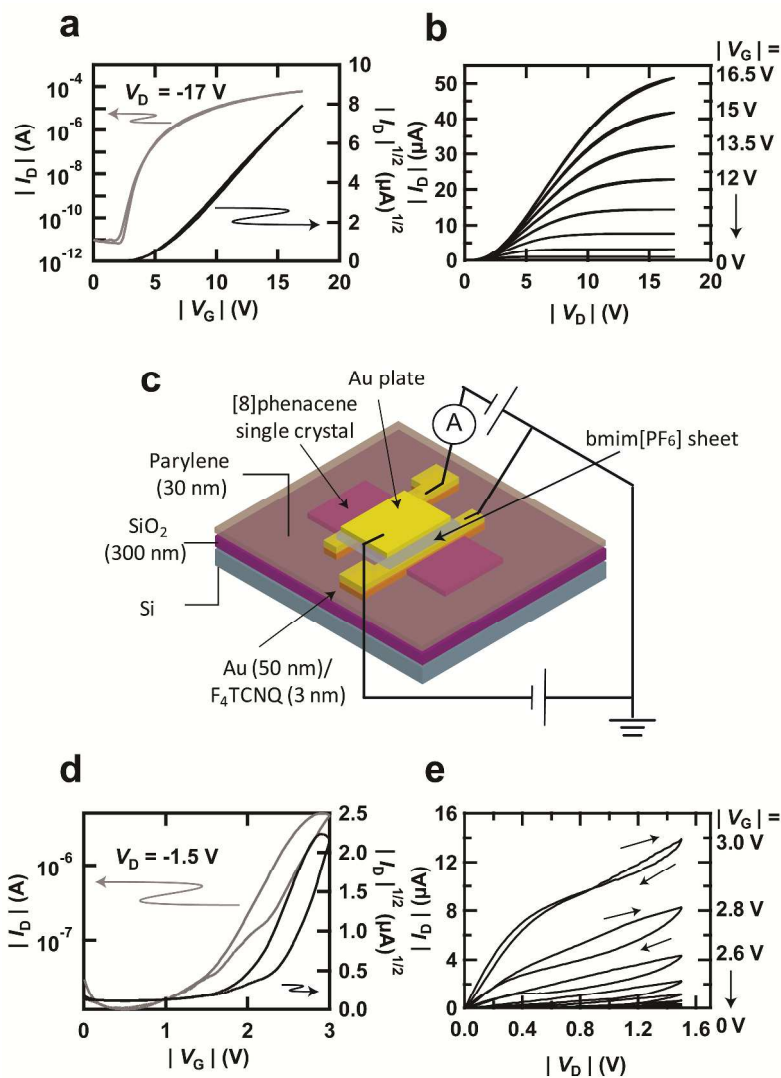


Fig. 5 (a) Transfer and (b) output curves of [8]phenacene single-crystal FET with PZT gate dielectrics measured in two-terminal measurement mode. (c) Schematic representation of two-terminal measurement mode and device structure of [8]phenacene single-crystal EDL FET. The EDL polymer sheet is rendered in grey. Gating is done through the Au plate on the EDL polymer sheet. (d) Transfer and (e) output curves of [8]phenacene single-crystal EDL FET with bmim[PF₆] polymer sheet measured in two-terminal measurement mode.

low, but this is the first demonstration of logic gate circuit using phenacene molecules. Very recently, we succeeded in fabrication of inverter circuit using [6]phenacene and *N,N'*-bis(*n*-octyl)-*x,y*, dicyanoperylene-3,4:9,10-bis(dicarboximide) (PDI8-CN₂) thin-film FETs, which shows G_{inverter} as high as 25 and $V_{\text{TIC}} = V_{\text{DD}}/2$,²⁶ suggesting the potential application of phenacene molecules towards logic gate circuit.

Discussion

In this study, a high-performance FET was realized with a single-crystal of [8]phenacene, which gave $\langle\mu\rangle$ values of 8.2 cm² V⁻¹ s⁻¹ with SiO₂ gate dielectrics. The excellent characteristics of the [8]phenacene single-crystal FET are

comparable to those in the [7]phenacene single-crystal FET, showing that single-crystal [8]phenacene is promising for FET application. Low-voltage operation of an [8]phenacene single-crystal FET with PZT gate dielectrics was achieved; the minimum $|V_{\text{th}}|$ in the FETs with PZT gate dielectrics was 3.5 V.

For a comparison of properties in the FET devices, the average values of μ , $|V_{\text{th}}|$, on-off ratio and S for each FET device fabricated in this study are listed in Table 1. As seen from Table 1, the $\langle\mu\rangle$ value, 3(2) cm² V⁻¹ s⁻¹, recorded in [8]phenacene single-crystal FET with SiO₂ gate dielectric is higher than that, 1.2(3) cm² V⁻¹ s⁻¹, in its thin-film FET. This suggests the similarity to [7]phenacene single-crystal FET which also provides the higher μ than that of its thin-film FET^{17,20,27}

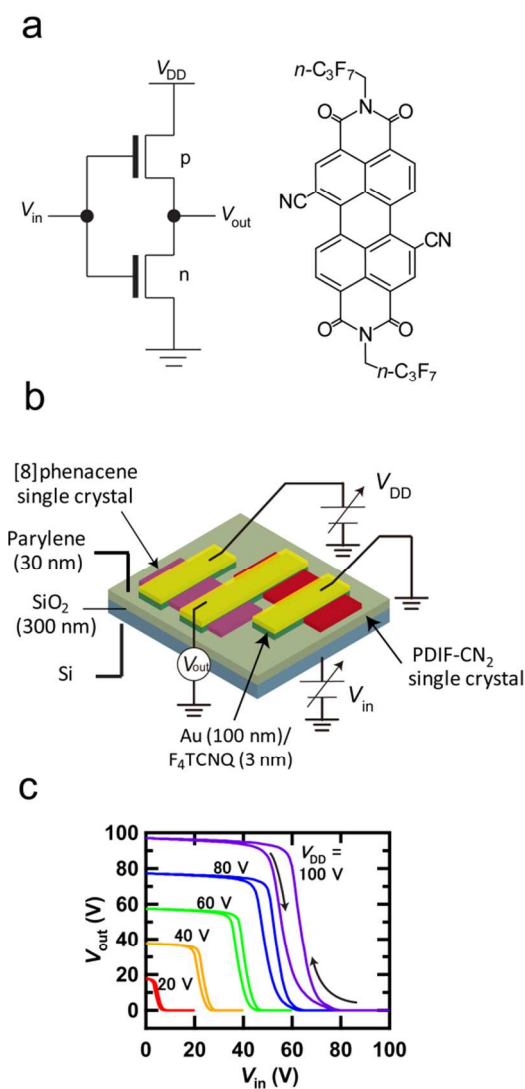


Fig. 6 (a) Constitution of CMOS inverter circuit and molecular structure of PDIF-CN₂, (b) schematic representation of inverter and measurement mode, (c) V_{out} – V_{in} plot at different V_{DD} 's of the inverter device using [8]phenacene and PDIF-CN₂ single-crystal FETs.

The optical micrograph images of single crystals of [7]phenacene (Fig. 1c of ref. 17) and [8]phenacene (Fig. 1a of this paper) show a very beautiful shape without defects and aggregates, contrary to the image of [6]phenacene (Fig. 1c of ref. 17). This is self-consistent with the high μ values in [7]phenacene and [8]phenacene single-crystal FETs.

In Fig. 7, the maximum μ value, μ_{max} , was plotted as a function of the number of benzene rings in each molecule. Here, it should be noticed that the FET properties would depend on geometry and structure of FET devices fabricated, in particular the orientation of ab -plane of single crystal. However, the graph shown in Fig. 7 is reliable since the behaviour that the μ_{max} increases with increasing number of benzene rings is determined based on the properties of many FETs. Because many FET devices using each phenacene molecule were fabricated and their FET properties were

evaluated, it can be expected that the most suitable single-crystal is found and it would provide the highest μ value (μ_{max}). For this reason, the μ_{max} would be associated with the intrinsic nature of [n]phenacene single-crystal FETs. Therefore, we will systematically discuss the FET properties of different phenacenes based on the behaviour of μ_{max} against number of benzene rings.

Table 1. Averaged FET parameters of [8]phenacene FETs.

gate dielectric	$\langle\mu\rangle$ ($\text{cm}^2\text{V}^{-1}\text{s}^{-1}$)	$\langle V_{th} \rangle$ (V)	$\langle\text{ON/OFF}\rangle$	$\langle S\rangle$ (V/decade)
SiO ₂ ^(a)	3(2)	26(8)	$2(3) \times 10^8$	2(1)
SiO ₂ ^(b)	6(2)	47(14)	$2.1(7) \times 10^7$	1.3(5)
PZT ^(a)	1.6(4)	5(1)	$5(5) \times 10^6$	1(1)
EDL ^(a)	$4(2) \times 10^{-1}$	2.38(4)	$7(13) \times 10^6$	$4(2) \times 10^{-1}$
SiO ₂ ^(c)	1.2(3)	39(7)	$2(2) \times 10^6$	3.9(8)

Evaluated for [8]phenacene single-crystal FETs in (a) two-terminal and (b) four-terminal measurement modes in this study. (c) FET parameters for [8]phenacene thin-film FETs in two-terminal measurement mode, which is taken from ref. 18.

As can be seen, the μ_{max} values are higher in the single-crystal FETs of [7]phenacene ($6.9 \text{ cm}^2 \text{ V}^{-1} \text{ s}^{-1}$)²⁰ and [8]phenacene ($8.2 \text{ cm}^2 \text{ V}^{-1} \text{ s}^{-1}$) than those in [6]phenacene ($5.6 \times 10^{-1} \text{ cm}^2 \text{ V}^{-1} \text{ s}^{-1}$)¹⁷ and picene ($1.3 \text{ cm}^2 \text{ V}^{-1} \text{ s}^{-1}$)¹⁹. Here, it is worth noting that the μ_{max} of [6]phenacene is lower than $1 \text{ cm}^2 \text{ V}^{-1} \text{ s}^{-1}$. The optical microscope image of [6]phenacene (Fig. 1c in ref. 17) shows an aggregation of many small crystals, and its flat area is too small in comparison with those of picene, [7]phenacene (Fig. 1c in ref. 17) and [8]phenacene (Fig. 1a of this paper). As described previously, the crystal shapes of [7]phenacene¹⁷ and [8]phenacene are similar (Fig. 1a). As c expands along with the number of benzene rings in each molecule, thin plate-like single crystals should tend to be formed because the two-dimensionality (2D) increases with the difference between a (or b) and c . This is desirable for FET operation because the ab -plane shows large transfer integrals between molecules as they become parallel to the gate dielectric; channel conduction occurs in the ab -plane as in other phenacene molecules^{17,19,20}, judging from the lattice constants and space group.

The expansion of c value causes difficulty of obtaining the single crystals with sufficient size to perform the single crystal XRD diffraction. We tried to collect sufficient Bragg diffraction data from the thin single-crystals of [8]phenacene, but the structural analysis has never succeeded. Namely, the structural information such as the exact orientation of molecules and the molecule-molecule distance has never been obtained. Therefore, the transfer integral between molecules have not been calculated for [8]phenacene solids. [n]phenacenes ($n > 5$) are still under this situation, and the

correlation between μ and transfer integral has not yet been clarified.

The fact that [7]phenacene and [8]phenacene single-crystal FETs show higher μ values than the smaller members of the group implies that the extension of the π -framework increases channel conductance, suggesting that the increase in π - π interaction between the molecules through the extension of the π -framework (phenacene core) does not conflict with the C-H...C interaction and leads directly to the increased transfer integral between molecules. The complete XRD measurements using single crystals are required for confirming the increased transfer integral between molecules in increasing number of benzene rings. For this purpose, the single-crystal XRD measurements with synchrotron X-ray beam would be indispensable.

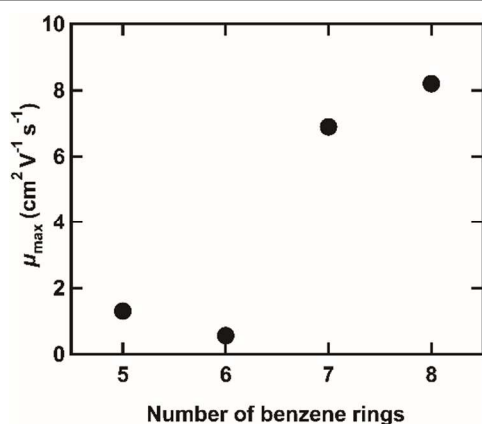


Fig. 7 Plot of μ_{\max} vs. number of benzene rings in phenacene single-crystal FETs.

Before this study, we expected an odd-even effect (parity-effect) on the μ value in phenacene single-crystal FETs because the [6]phenacene single-crystal FET showed a very low μ value ($\mu_{\max} = 5.6 \times 10^{-1} \text{ cm}^2 \text{ V}^{-1} \text{ s}^{-1}$) in comparison with those of picene¹⁹ and [7]phenacene²⁰. However, the odd-even effect was completely contradicted, as seen from Fig. 7. Instead, the channel conductance is enhanced by the increase in π - π interaction due to extension of the π -framework. At least up to [8]phenacene, factors other than the increased π - π interaction do not provide any negative influence on FET properties. Simply put, increasing the number of benzene rings increases the μ value in phenacene single-crystal FETs.

Conclusions

The FET operation of [8]phenacene single-crystal FET devices was fully investigated, and the high μ value ($> 8 \text{ cm}^2 \text{ V}^{-1} \text{ s}^{-1}$) was obtained. In this paper, the parameters obtained from FET devices are recorded and the average μ values are utilized to compare the FET performance of [8]phenacene single-crystal FET with that of other organic FETs. The low voltage operation was also achieved using high- k gate dielectric and EDL capacitor. Furthermore, the fabrication and operation of inverter circuit using [8]phenacene single-crystal FET was successfully

demonstrated. The G_{inverter} of the inverter circuit is still low, but the successful operation may open a new avenue for future high-performance / practical logic gate circuits using phenacene molecules. Actually, the most important point to realize high G_{inverter} is to search for n-channel organic FETs balanced to [8]phenacene FET; as seen from Fig. S3, the S and on-off ratio in PDIF-CN₂ (14 V decade^{-1} and 1.8×10^2) is poor in comparison with those of typical [8]phenacene single-crystal FET.

In this study, we pursued the correlation between μ and number of benzene rings in phenacene single-crystal FETs. Our conclusion on this point is that strengthened π - π interaction through the increased number (or extension of π -framework) is a key for enhancement of μ value. Further investigation using more extended phenacene molecules such as [9]phenacene and [10]phenacene would clarify whether the μ value increases more with the number of benzene rings or saturates. This is very significant for clarifying the strategy to design extended π -network materials available to organic electronics.

Experimental section

Sample preparation and characterization of FET devices

An [8]phenacene sample was synthesized and characterised by our group (details in ref. 18), and a PDIF-CN₂ sample was purchased from Polyera Active Inc. The XRD pattern of an [8]phenacene powder sample and a thin film showed that the sample was in fact [8]phenacene. Single crystals of [8]phenacene and PDIF-CN₂ were prepared using the PVT method, using the equipment shown in Fig. S10 of ref. 18 and Fig. 5 of ref. 23. The sample was loaded in the high-temperature zone (430°C for [8]phenacene and 400°C for PDIF-CN₂), and the single crystals were collected in the low-temperature zone (280°C for [8]phenacene and 330°C for PDIF-CN₂). The Ar gas flow was 70 ml min^{-1} . Each obtained single crystal was loaded on a substrate for fabricating an FET device. XRD and AFM were measured using X-ray diffractometers (RIGAKU RINT-TTR III for powder samples and RIGAKU SMARTLAB-PRO for thin films) with Cu K α source (wavelength of 1.5418 \AA) and an AFM measurement system (SII Nano Technology SPA400), respectively.

For the [8]phenacene and PDIF-CN₂ FET-device fabrication, 100-nm thick Au source / drain electrodes were formed on the single crystals by thermal evaporation under 10^{-7} Torr. 3-nm thick F₄TCNQ was inserted between single crystal and electrodes to reduce contact resistance. The EDL polymer sheet was made using bmim[PF₆] and poly(vinylidene fluoride-co-hexafluoropropylene). Details are shown in Ref. 18. The FET characteristics were measured using a semiconductor parameter analyser (Agilent B1500A). The capacitance for gate dielectrics was directly measured using a precision LCR meter (Agilent E4980A). The C_0 used for analysis of FET-performance was determined by extrapolation of the

capacitance measured at 20 Hz – 1 kHz to 0 Hz. The C_0 of each gate-dielectric at 0 Hz is as follows: $C_0 = 10.4 \text{ nF cm}^{-2}$ for parylene-coated SiO_2 (300 nm), $C_0 = 8.62 \text{ nF cm}^{-2}$ for HMDS-coated SiO_2 (400 nm), $C_0 = 62.5 \text{ nF cm}^{-2}$ for parylene-coated PZT (150 nm), and $C_0 = 7.86 \text{ } \mu\text{F cm}^{-2}$ for EDL polymer sheet. The methods of gating and measurement of I_D are explained in Fig. 2a, 4a and 5c. The L and W for each FET device were listed in Tables S2 – S5 of ESI†.

Acknowledgements

This study was partly supported by Grants-in-Aid (22244045, 26105004 and 24550054) from MEXT, from the LEMSUPER project (JST-EU Superconductor Project) of the Japan Science and Technology Agency (JST), and by the Program for Promoting the Enhancement of Research Universities. A.C. acknowledges the support by the Italian MIUR through Progetto Premiale 2012 EOS: organic electronics for advanced research.

Notes and references

- ^a Department of Electric and Electronic Engineering, Okayama University, Okayama 700-8530, Japan
- ^b Research Laboratory for Surface Science, Okayama University, Okayama 700-8530, Japan
- ^c Department of Chemistry, Okayama University, Okayama 700-8530, Japan
- ^d NARD Co. Ltd. Amagasaki 660-0805, Japan
- ^e CNR-SPIN and Department of Physics, University of Naples, Piazzale Tecchio 80, 80125, Naples, Italy
- ^f Research Centre of New Functional Materials for Energy Production, Storage and Transport, Okayama University, Japan
- ^g Japan Science and Technology Agency, ACT-C, 4-1-8 Honcho, Kawaguchi, Saitama, 332-0012, Japan

† Electronic Supplementary Information (ESI) available: [‘lattice constants of phenacene crystals, all FET parameters determined in this study and L dependence of μ in [8]phenacene single-crystal FET with SiO_2 gate dielectric, and transfer / output curves of [8]phenacene single-crystal FET with HMDS-coated SiO_2 gate dielectric’ should be included here].

See DOI: 10.1039/b000000x/

- 1 J. Takeya, C. Goldmann, S. Haas, K. P. Pernstich, B. Ketterer, B. Batlogg, *J. Appl. Phys.*, 2003, **94**, 5800-5804.
- 2 V. Podzorov, S. E. Sysoev, E. Loginova, H. V. M. Pudalov and M. E. Gershenson, *Appl. Phys. Lett.*, 2003, **83**, 3504-3506.
- 3 J. Takeya, M. Yamagishi, Y. Tominari, R. Hirahara, Y. Nakazawa, T. Nishikawa, T. Kawase, T. Shimoda and S. Ogawa, *Appl. Phys. Lett.*, 2007, **90**, 102120.
- 4 Y. Kawasaki, H. M. Yamamoto, M. Hosoda, N. Tajima, T. Fukunaga, K. Tsukagoshi and R. Kato, *Appl. Phys. Lett.*, 2008, **92**, 243508.
- 5 K. P. Pernstich, S. Haas, D. Oberhoff, C. Goldmann, D. J. Gundlach, B. Batlogg, A. N. Rashid and G. Schitter, *J. Appl. Phys.*, 2004, **96**, 6431-6438.
- 6 C. Reese and Z. Bao, *Mater. Today*, 2007, **10**, 20-27.
- 7 O. D. Jurchescu, M. Popinciuc, B. J. van Wees and T. T. M. Palstra, *Adv. Mater.*, 2007, **19**, 688-692.
- 8 C. Liu, T. Minari, X. Lu, A. Kumatani, K. Takimiya and K. Tsukagoshi, *Adv. Mater.*, 2011, **23**, 523-526.
- 9 A. N. Sokolov, S. A-Evrenk, R. Mondal, H. B. Akkerman, R. S. S.-Carrera, S. G.-Focil, J. Schrier, S. C. B. Mannsfeld, A. P. Zoombelt, Z. Bao and A. A.-Guzik *Nature Commun.*, 2011, **2**, 437.
- 10 D. T. Chase, A. G. Fix, S. J. Kang, B. D. Rose, C. D. Weber, Y. Zhong, L. N. Zakharov, M. C. Lonergan, C. Nuckolls, M. M. Haley, *J. Am. Chem. Soc.*, 2012, **134**, 10349-10352.
- 11 J. Mei, Y. Diao, A. L. Appleton, L. Fang, Z. Bao, *J. Am. Chem. Soc.* 2013, **135**, 6724-6746.
- 12 Y. Yuan, G. Giri, A. L. Ayzner, A. P. Zoombelt, S. C. B. Mannsfeld, J. Chen, D. Nordlund, M. F. Toney, J. Huang and Z. Bao, *Nature Commun.*, 2014, **5**, 3005.
- 13 H. Okamoto, S. Hamao, H. Goto, Y. Sakai, M. Izumi, S. Gohda, Y. Kubozono and R. Eguchi, *Sci. Rep.*, 2014, **4**, 5048.
- 14 H. Okamoto, N. Kawasaki, Y. Kaji, Y. Kubozono, A. Fujiwara and M. Yamaji, *J. Am. Chem. Soc.*, 2008, **130**, 10470-10471.
- 15 N. Kawasaki, Y. Kubozono, H. Okamoto, A. Fujiwara and M. Yamaji, *Appl. Phys. Lett.*, 2009, **94**, 043310.
- 16 R. Eguchi, X. He, S. Hamao, H. Goto, H. Okamoto, S. Gohda, K. Sato and Y. Kubozono, *Phys. Chem. Chem. Phys.*, 2013, **15**, 20611-20617.
- 17 X. He, R. Eguchi, H. Goto, E. Uesugi, S. Hamao, Y. Takabayashi and Y. Kubozono, *Org. Electron.*, 2013, **14**, 1673-1682.
- 18 H. Okamoto, R. Eguchi, S. Hamao, H. Goto, K. Gotoh, Y. Sakai, M. Izumi, Y. Takaguchi, S. Gohda and Y. Kubozono, *Sci. Rep.*, 2014, **4**, 5330.
- 19 N. Kawai, R. Eguchi, H. Goto, K. Akaike, Y. Kaji, T. Kambe, A. Fujiwara and Y. Kubozono, *J. Phys. Chem. C*, 2012, **116**, 7983-7988.
- 20 X. He, S. Hamao, R. Eguchi, H. Goto, Y. Yoshida, G. Saito and Y. Kubozono, *J. Phys. Chem. C*, 2014, **118**, 5284-5293.
- 21 R. Mitsuhashi, Y. Suzuki, Y. Yamanari, H. Mitamura, T. Kambe, N. Ikeda, H. Okamoto, A. Fujiwara, M. Yamaji, N. Kawasaki, Y. Maniwa and Y. Kubozono, *Nature*, 2010, **464**, 76-79.
- 22 S. M. Sze, *Semiconductor devices, Physics and Technology*, John Wiley & Sons. Inc., New York, 2nd edn, 1985.
- 23 Y. Kubozono, X. He, S. Hamao, K. Teranishi, H. Goto, R. Eguchi, T. Kambe, S. Gohda and Y. Nishihara, *Eur. J. Inorg. Chem.*, 2014, **24**, 3806-3819.
- 24 F. Chiarella, T. Toccoli, M. Barra, L. Avaersa, F. Ciccullo, R. Tatti, R. Verucchi, S. Iannotta and A. Cassinese, *Appl. Phys Lett.*, 2014, **104**, 143302.
- 25 M. Barra, F. V. Di Girolamo, N. A. Minder, I. G. Lezama, Z. Chen, A. Facchetti, A. F. Morpurgo and A. Cassinese, *Appl. Phys. Lett.* 100, 133301 (2012).
- 26 T. Mikami, Y. Shimo, H. T. Murakami, H. Hamao, H. Goto, R. Eguchi, Y. Hayashi, and Y. Kubozono, *unpublished data*.

- 27 Y. Sugawara, Y. Kaji, K. Ogawa, R. Eguchi, S. Oikawa, H. Gohda, A. Fujiwara and Y. Kubozono, *Appl. Phys. Lett.*, 2011, **98**, 013303.

Transistor application of single crystals of [8]phenacene

Yuma Shimo, Takahiro Mikami, Hiroto T. Murakami, Shino Hamao, Hidenori Goto, Hideki Okamoto, Shin Gohda, Kaori Sato, Antonio Cassinese, Yasuhiko Hayashi and Yoshihiro Kubozono

J. Mater. Chem., 2014, **xx**, xxxx-xxxx.

DOI: 10.1039/C2JMxxxxx

Field-effect transistors have been fabricated that use [8]phenacene single-crystals, showing the maximum μ value of $8.2 \text{ cm}^2 \text{ V}^{-1} \text{ s}^{-1}$. The CMOS inverter circuit has also been fabricated, which is the first step for future practical electronics.

